SSEC NO.76.11.S1

GATE AREA RAINFALL ESTIMATION FROM GEOSTATIONARY SATELLITE IMAGES-- PRELIMINARY RESULTS

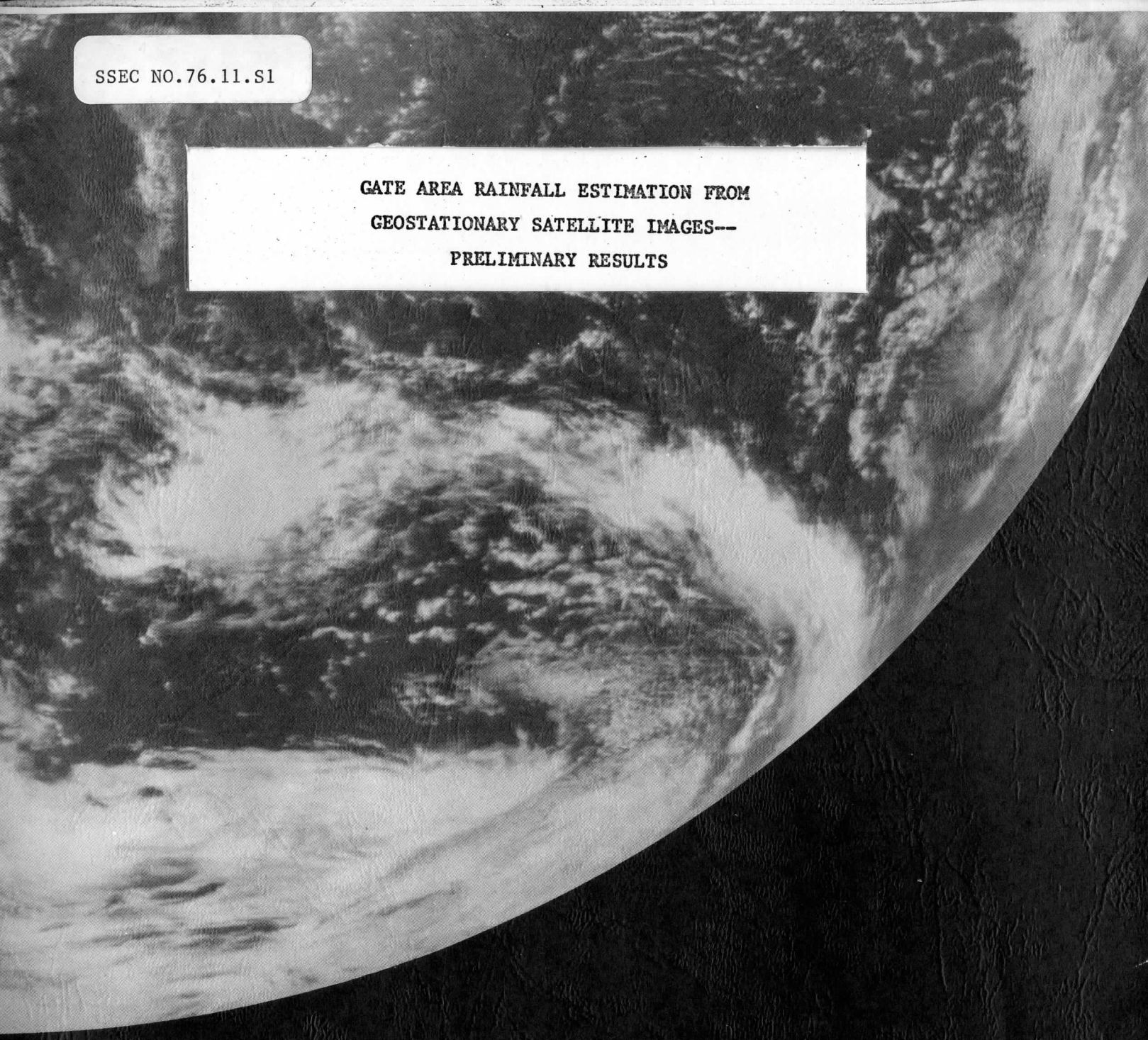

A REPORT

from the space science and engineering center
the university of wisconsin-madison
madison, wisconsin

GATE AREA RAINFALL ESTIMATION FROM GEOSTATIONARY SATELLITE IMAGES-- PRELIMINARY RESULTS

A report on NOAA Grant 04-5-158-47

John Stout
David W. Martin

Space Science and Engineering Center
University of Wisconsin
1225 West Dayton Street
Madison, Wisconsin 53706

Dhirendra N. Sikdar

Geological Sciences Department
University of Wisconsin
3409 North Downer Street
Milwaukee, Wisconsin 53201

November 1976

TABLE OF CONTENTS

ACKNOWLEDGEMENTS

Steve Hentz and Cecil Lo assisted in data analysis. Figures were capably drafted by Tony Wendricks. Mrs. Barbara Mueller typed the text.

This program was carried out in collaboration with Cecelia Griffith and William Woodley of NOAA's National Hurricane and Experimental Meteorology Laboratory.

I. Introduction

Several years ago Sikdar (1972) found expansion of the cirrus canopy atop deep convective clouds to be a measure of volumetric rainfall. More recently Griffith and Woodley (1975) and Reynolds and Von der Haar (1975) confirmed a positive relationship between convective cloud thickness and cloud brightness. To the extent that cloud thickness is proportional to rainfall, this latter finding suggests rainfall also is related to brightness. Indeed, this has been found to be true, for example, when radar echoes are compared with satellite clouds (Martin and Suomi, 1971; Woodley and Sancho, 1971; Woodley, Sancho, and Miller, 1972), but the association with rainfall is best for growing clouds, that is, deep convective clouds in early and mature stages of development (Martin and Sikdar, 1973, 1974; Griffith et al., 1976).

These time dependent relationships of brightness, area, and rainfall form the basis for a method to estimate convective rainfall from images of geostationary satellites. This report summarizes the method, and describes work done over the past year: procedures, results of GATE measurements, a consolidation of GATE and Florida results, and results from a limited test for one GATE day.

II. Method

We suppose that for a deep convective cloud in a given state of development, area measured from a satellite picture is proportional to volumetric rainfall. To establish this proportionality we identify a number of deep convective clouds, then measure their areas and--from calibrated radars--the rainfall they produce. Both visible and infrared satellite image sequences are used. Visible images offer better spatial resolution and a

more penetrating view of clouds; infrared images provide continuous day and night coverage.

Use of sequences simplifies the problem of discriminating between convective clouds and layer clouds, which in the tropical regions for which the method is designed apparently contribute little to total precipitation. (The latter point is discussed in Section V below.) In visible wavelengths discrimination is based on brightness. In infrared wavelengths another primary criterion is needed: not only are deep convective clouds bright, they expand, sometimes explosively. (Discrimination is aided by a host of secondary criteria, such as shape, texture, organization, movement, and background cloudiness.)

Measurements of cloud area are made on McIDAS, a digital image access and processing system with video display (a user's description is given in Chatters and Suomi, 1975). Cloud entities are identified in a satellite image sequence. Outlines for a single picture then are drawn with an operator controlled cursor. The computer records these outlines and the cloud area within them above operator specified threshold brightnesses. When all clouds are all outlined, the operator steps to the next picture, and so on through the sequence.

Rainfall associated with the outlined clouds is calculated in three steps. Digital radar images first are remapped to satellite projection. The remapped images then are displayed on McIDAS, opposite the satellite sequence. Echo area at various intensity levels is measured, in the same way cloud area is, from outlines drawn to match cloud outlines. These echo areas then are converted through an appropriate reflectivity-rainfall relation to volumetric rain rates, and summed to obtain the total cloud volumetric rain rate. Details of this procedure are given in Appendix B.

These sequences of area and rainfall for individual clouds can be combined if they are first normalized by size. Cloud area (A_c) and volumetric rainfall (V) are divided by maximum cloud area ($A_{c\ max}$). The average of many such normalized curves produces the relation used to estimate rainfall. Two of these average relations can be established, one for clouds viewed in infrared wavelengths (Fig. 1), one for clouds viewed in visible wavelengths (Fig. 2).

The use of these relations to estimate rainfall is as follows: Measure area over the lifetime of a cloud. Divide each area measurement by maximum cloud area. Enter the cloud area-rainfall curve on the cloud area axis, read normalized rain rate, and multiply by maximum cloud area to obtain the rain estimate as a volumetric rate.

III. Status

Sequences from eight days have been analyzed (Table I). Seven day-sequences, including two in the GATE area, were used to establish the normalized cloud area-rainfall curves. The eighth is our test production case, a 20° by 20° box in the GATE area on 5 September 1974.

IV. Development of GATE Area Relation

The relationship developed previously for clouds over south Florida was extended to the GATE area through measurements of cloud area and rainfall in the vicinity of the U.S. ship Oceanographer, stationed during Phase III at 07°45'N, 22°12'W. Three steps are involved: measurements of cloud area and rainfall, area normalization of those measurements, and their combination into a relation appropriate for estimating rainfall in GATE.

Twenty-six visible and 47 infrared cloud-echo pairs were measured on SMS sequences from the 4th and 6th of September 1974. Sample plots of cloud area, echo area, and rainfall are shown in Fig. 3. These curves are similar

TABLE 1

YEAR	JULIAN DAY	CALENDAR DAY	SATELLITE	LOCATION	VISIBLE number of clouds	VISIBLE hours time span	INFRARED number of clouds	INFRARED hours time span
1973	178	27 June	ATS	South Florida	13	7	--	--
1973	183	2 July	ATS	South Florida	7	6	--	--
1973	222	10 Aug.	ATS	South Florida	15	6	--	--
1974	216	4 Aug.	SMS	South Florida	14	7 1/2	9	7 1/2
1974	248	5 Sept.	SMS	South Florida	9	6 1/2	13	8 1/2
1974	247	4 Sept.	SMS	GATE	15	6	36	19 1/2
1974	249	6 Sept.	SMS	GATE	11	6	11	13 1/2
1974	248	5 Sept.	SMS	GATE	--	--	65	11 1/2

to those for clouds over south Florida. In particular, rainfall peaks earlier than cloud area, with most of the rain occurring before the cloud reaches its maximum area. The main disadvantage of visible data is illustrated in the second of these plots: often only part of the cloud life cycle is captured. Coverage is limited to three hours either side of local noon, even with brightness normalization for changing sun-cloud-satellite geometry.

Distributions of area normalized cloud and volumetric rainfall measurements are displayed in Fig. 4. This diagram shows all such points from the two GATE days. Since many infrared clouds were not detected until after the onset of precipitation, the infrared points begin high relative to the visible points. The flatter infrared distribution is due in part to a sharper peak and longer decay period than in the visible (stretching the rain over a greater range of normalized cloud area values). There also is greater variability in the phase relation between rain and cloud area maxima.

To compare different synoptic conditions, satellites, and geographical area, averages for each day were calculated. The infrared curves, in Fig. 5, are basically alike for each day. The clouds from these four days were averaged and a smooth curve drawn through them to produce the combined infrared working relation shown in Fig. 1.

The visible day-averaged curves, seen in Fig. 6, showed larger differences between the days. The average of the three ATS days has a much higher rain to cloud area ratio than the four SMS days. This may be partly due to generally poorer data and data processing. (ATS had coarser resolution and less control of signal gain than does SMS. Techniques, by present standards, were primitive when the ATS images were processed.) The equivalencing between ATS and SMS levels may also be a factor. On the basis of curves

shown in Fig. 7 it had been concluded that an ATS-3 digital count of 60 was equivalent to an SMS-1 count of 172 (Martin, Stout, and Sikdar, 1975). If the true SMS equivalent count was higher than 172, then the present rain to cloud area ratio would be too small relative to the same ratio for ATS. The effect of a higher SMS equivalence level is shown in Fig. 8. Use of this level (184) would only account for a small part of the ATS-SMS discrepancy in rain-cloud area ratios. Still another factor is the effect of shear. Marwitz (1972) and Foote and Fankhauser (1973) noted an inverse relation between vertical shear of the horizontal wind and precipitation efficiency. A plot of wind shear (measured over the layer 850 mb to 200 mb) against the ratio of maximum rain to cloud area (Fig. 9) shows the expected inverse relation, except for the low shear day 73178. (Even this point is not inconsistent with Foote and Fankhauser (1973) who found greater variability in lower shears.)

Because the source of this difference remains uncertain, it seems prudent to base the GATE area rainfall relation only on SMS data. This relation is shown in Fig. 2.

V. Refinements

The method as we have described it applies to deep convective clouds having lifetimes that are long compared to the interval between pictures. It neglects rain from small cumulus, small congestus, and stratiform clouds. We have estimated the amount of this rain using the sequence of Oceanographer radar images for 4 September. An outline was drawn around all echoes corresponding to measured clouds, and unmeasured cumulus, congestus, and layered clouds. Only deep convective clouds that were unmeasured due to area or time truncation were excluded. The rain falling within the outline was compared to the sum

of rain falling from measured clouds. The fraction of rain missed by our measurements varied from 22% to 3% (Fig. 10). As convection became more organized the missed fraction declined. We conclude that this method may overlook, especially in convectively less organized situations, as much as 1/4 of the total area rainfall.

A simple technique is proposed to account for this rain. A grid will be drawn on the unmeasured sections of the satellite image. The area above a threshold brightness within each grid box will be measured, and multiplied by a constant to obtain a grid rain estimate. The threshold and the visible and infrared constants will be derived by comparing the cloud area and radar measured rainfall of grid boxes from the calibration days, 4 and 6 September.

VI. Test Case

The test of the GATE area cloud area-rainfall relation serves two purposes: first, to verify the method for fixed areas; and, second, to define and resolve problems that may be encountered in production cases. These problems include working with a large area, assigning rainfall to the proper area, and determining a format for presenting results.

Our test case is 5 September 1974; the area a 20° by 20° box centered on the middle of the GATE B-array (08°30'N, 23°30'W). Sixty-five clouds were measured from 04 to 15 GMT, using full resolution infrared data. Plots of area for sample clouds are shown in Fig. 11.

Production estimates will be presented in map and table form, one map and one table per satellite image. Fig. 12 is a sample map from the 5 September test. Circles whose area on the map is proportional to rain volume are plotted at the position of maximum cloud brightness. Table 2 gives information on position and rainfall for the time of the map.

TABLE 2

RAINFALL ESTIMATION FOR 18 SEPTEMBER 1974

TIME	TOTAL	INDIVIDUAL CLOUDS											
1300	46088	9	166	12	1523	15	184	18	8	31	4753	34	226
			833		940		922		912		937		657
			-2021		-2122		-2338		-2658		-1946		-1620
		36	22	37	442	41	18305	42	1038	44	19	45	353
			546		1100		850		850		630		1108
			-2755		-2041		-2511		-2240		-2557		-1939
		46	7507	48	744	49	1759	51	3611	52	13	56	403
			850		526		907		610		520		1016
			-2121		-2658		-2049		-1631		-2743		-2747
		58	110	59	30	60	2740	61	181	62	1951		
			501		427		1100		620		824		
			-2627		-2622		-2041		-2518		-2052		

Key to individual clouds: CC RAIN where CC = cloud number
LAT RAIN = volumetric rainfall rate in $m^3 s^{-1}$
LON LAT = latitude in degrees and minutes
LON = longitude in degrees and minutes

To assign clouds and cloud fractions to fixed areas (in this test case the four quadrants of the Oceanographer radar), the boundaries of the area were drawn on the 5 September rainfall maps. The fraction of the cloud's circle inside the boundary was taken as the fraction of that cloud's rain falling inside the area. These fractional volumetric rainfall rates were summed to get a quadrant rainfall, which was then compared with rainfall calculated from digital radar data for the four quadrants. Neglecting quadrants III and IV, which had little rain (1% of the quadrant I and II total rainfall over the verification period), the half hour estimates were 50-100% of the observed rain (Fig. 13). The major exception occurred from 0900 to 1000 Z when a very large cloud was on the border of quadrant II. The underestimation of two to three times points out the need for an assignment of variability as a function of the number and size distribution of clouds. It also suggests that individual treatment of very large clouds could improve our estimates. Brightness gradient, texture (Oliver and Scofield, 1976), and contour areas at higher levels (Griffith et al., 1976) may be useful. The sum of the rain estimates for the four quadrants over the verification period (600-1000 Z) was 80% of the observed rain. Some or all of the difference would be accounted for by the estimate of rain falling from layer clouds proposed in Section V.

VII. Summary and Plans

A GATE working relationship has been derived for visible and infrared data. A test of the infrared relation yielded a total rain estimate of 80% of observed rain, and closer to 100% if rain from layer clouds had been estimated.

The ground truth for this verification was the digital radar data of

the Oceanographer. These data are from an interim set, which was not corrected for possible beam absorption by the sea, atmospheric attenuation, rain attenuation (including rain on the radome), and non-beam filling (Hudlow, personal communication, 1976). These effects all contribute to a diminished estimate of rainfall, therefore, the estimates of volumetric rainfall rate in this report are likely to be less than true rainfall. The amount of the underestimate will be better known when raingage measurements have been compared with radar estimates, and corrections have been developed for the radar. This work is underway (Hudlow, personal communication, 1976).

Whether the remarkably good agreement of satellite and radar estimates for 5 September is a true measure of the accuracy inherent in this method or merely fortuitous remains to be seen. Certainly it encourages hope that the satellite can provide estimates of rainfall able to meet even the exacting demands of budget analyses.

Plans for the next few months include

1. Refinements to method. We plan to

-- update present rain relations and estimates as more accurate ground truth data are provided,

-- develop a simple rain estimation technique for small cumulus and layer clouds,

-- further automate and improve the rain estimation procedure.

2. Production. Rain estimates will be made for 5-10 days, most from the 1977 NCAR Workshop priority period 1-12 September 1974. Results will be presented in map and table form, one map and one table per satellite image. In contrast to those of the test case, circles will be drawn with map area proportional to cloud area. The average rainfall over that area

will be written in the circle. Fig. 14 shows a hand drawn version.

Production maps will be created on a Cal Comp Plotter.

REFERENCES

Austin, P., S. Geotis, J. Cunning, J. Thomas, and R. Sax, 1976: Raindrop Size Distributions and Z-R Relationships for GATE. Paper presented at the 10th AMS Technical Conference on Hurricanes and Tropical Meteorology, July 6-9, 1976, Charlottesville, VA.

Chatters, G. C. and V. E. Suomi, 1975: The Applications of McIDAS. IEEE Transactions on Geoscience Electronics, GE-13, 137-146.

Foote, G. B. and J. C. Fankhauser, 1973: Airflow and Moisture Budget Beneath a Northeast Colorado Hailstorm. J. Appl. Meteor., 12, 1330-1353.

Griffith, C. G. and W. L. Woodley, 1973: On the Variation with Height of the Top Brightness of Precipitating Convective Clouds. J. Appl. Meteor., 12, 1086-1089.

Griffith, C. G., W. L. Woodley, S. Browner, J. Teijeiro, M. Maier, D. W. Martin, J. Stout, and D. N. Sikdar, 1976: Rainfall Estimation from Geosynchronous Satellite Imagery During Daylight Hours. NOAA Tech. Rep. ERL 356-WMPO 7, 106 pp.

Martin, D. W. and V. E. Suomi, 1972: A Satellite Study of Cloud Clusters Over the Tropical North Atlantic Ocean. Bull. Amer. Meteor. Soc., 53, 135-156.

Martin, D. W. and D. N. Sikdar, 1973: Calibration of ATS-3 Images for Quantitative Precipitation Estimation. Report on NOAA Contract 03-3-022-18, Space Science and Engineering Center, Univ. of Wisconsin, Madison.

Martin, D. W. and D. N. Sikdar, 1974: Rainfall Estimation From Satellite Images. Report on NOAA Contract 03-4-022-22, Space Science and Engineering Center, Univ. of Wisconsin, Madison.

Martin, D. W., J. Stout, and D. N. Sikdar, 1975: GATE Area Rainfall Estimation From Satellite Images. Report on NOAA Grant 04-5-158-47, Space Science and Engineering Center, Univ. of Wisconsin, Madison.

Marwitz, J. D., 1972: Precipitation Efficiency of Thunderstorms on the High Plains. Preprints 3rd Conf. Wea. Modification, Rapid City, S. D., Amer. Meteor. Soc., 245-247.

Oliver, V. J. and R. A. Scofield, 1976: Estimation of Rainfall From Satellite Imagery. Preprints, Sixth Conference on Weather Forecasting and Analysis of the Am. Meteor. Soc., Albany, NY.

Reynolds, D. and T. H. Von der Haar, 1975: A Comparison of Radar Determined Cloud Height and Reflected Solar Radiance Measured From the Geosynchronous Satellite ATS-3. J. Appl. Meteor., 12, 1082-1085.

Sikdar, D. N., 1972: ATS-3 Observed Cloud Brightness Field Related to a Meso- to Subsynoptic-scale Rainfall Pattern. Tellus, 24, 400-413.

Woodley, W. L. and B. Sancho, 1971: A First Step Towards Rainfall Estimation From Satellite Cloud Photographs. Weather, 26, 279-289.

Woodley, W. L., B. Sancho, and A. H. Miller, 1972: Rainfall Estimation From Satellite Cloud Photographs. NOAA Technical Memorandum, ERL OD-11, 43 pp.

CAPTIONS TO FIGURES

Figure 1 Time dependent curve relating infrared cloud area (at 160 digital counts) to volumetric rainfall rate. Both cloud area and rainfall have been normalized by maximum cloud area. Normalized volumetric rainfall rate (V/A_c max) can be interpreted as an area averaged rain intensity. An intensity of 1 mm hr^{-1} would be .28 on this scale. Data points are averages for intervals on the cloud area axis 0.1 units in length. End point intervals are 0.05 units in length. Data are from four SMS days (see Table 1). This is the curve used to estimate rainfall from infrared pictures of the GATE area.

Figure 2 Time dependent curve relating visible cloud area (at 172 digital counts) to volumetric rainfall rate. This is the curve used to estimate rainfall from visible pictures of the GATE area. For further details, see Fig. 1.

Figure 3 Visible and infrared cloud area, echo area, and volumetric rainfall rate as a function of time. Clouds are from 6 September (top) and 4 September (bottom), in the vicinity of the Oceanographer.

Figure 4 Normalized cloud area and volumetric rainfall rate for GATE area infrared clouds (top) and visible clouds (bottom), 4 and 6 September 1974.

Figure 5 Day averages of infrared normalized cloud area and volumetric rainfall rate. Dates are indicated by YYDDD, where YY is the last two digits of the year, and DDD is the Julian day.

Figure 6 Day averages of visible normalized cloud area and volumetric rainfall rate.

Figure 7 ATS-3 brightness and equivalent SMS-1 visible channel brightness based on sensor and signal characteristics (dotted line) and measured for specific clouds (dashed and solid lines).

Figure 8 Normalized cloud area and volumetric rainfall rate at visible brightness threshold levels of 172 and 184 digital counts. Data are for 4 September 1974. (Some level 172 ordinate values are higher than corresponding level 184 ordinate values because of shifts in the abscissa values.)

Figure 9 The relationship of normalized volumetric rainfall rate to tropospheric shear. Each point represents an average of the maximum rain rate for all clouds on a given day. Tropospheric shear is the difference between 850 mb and 200 mb winds, as measured by proximate rawinsondes. F indicates a Florida case, G a GATE case.

Figure 10 The difference between satellite estimated and radar measured rainfall for the Oceanographer, expressed as a fraction of radar measured rainfall. The number of outlined clouds contributing to satellite estimates at each time is also shown as a measure of cloud organization. Data for 4 September 1974.

Figure 11 Infrared cloud area as a function of time for two clouds on 5 September 1974. Area is shown for four threshold brightness levels.

Figure 12 Rain estimation map for 1300 GMT, 5 September 1974. Estimates are plotted as circles for which area is proportional to the estimated volumetric rainfall rate.

Figure 13 Total rain estimates for the four quadrants of the Oceanographer radar compared with observed rainfall for 5 September. Note the difference in scales for volumetric rainfall rate between I, II and III, IV.

Figure 14 Same as Fig. 12, except the circles are drawn with area proportional to cloud area. Rainfall rate averaged over this area is entered as a number in m s^{-1} x 10^{-9} at the center of the cloud circle.

Figure 15 Average infrared normalized cloud area and rainfall. This relation was used for rain estimation for 5 September 1974. It is the same as Fig. 1 except that the rainfall calculations were made with the old Z-R relation (see Appendix A).

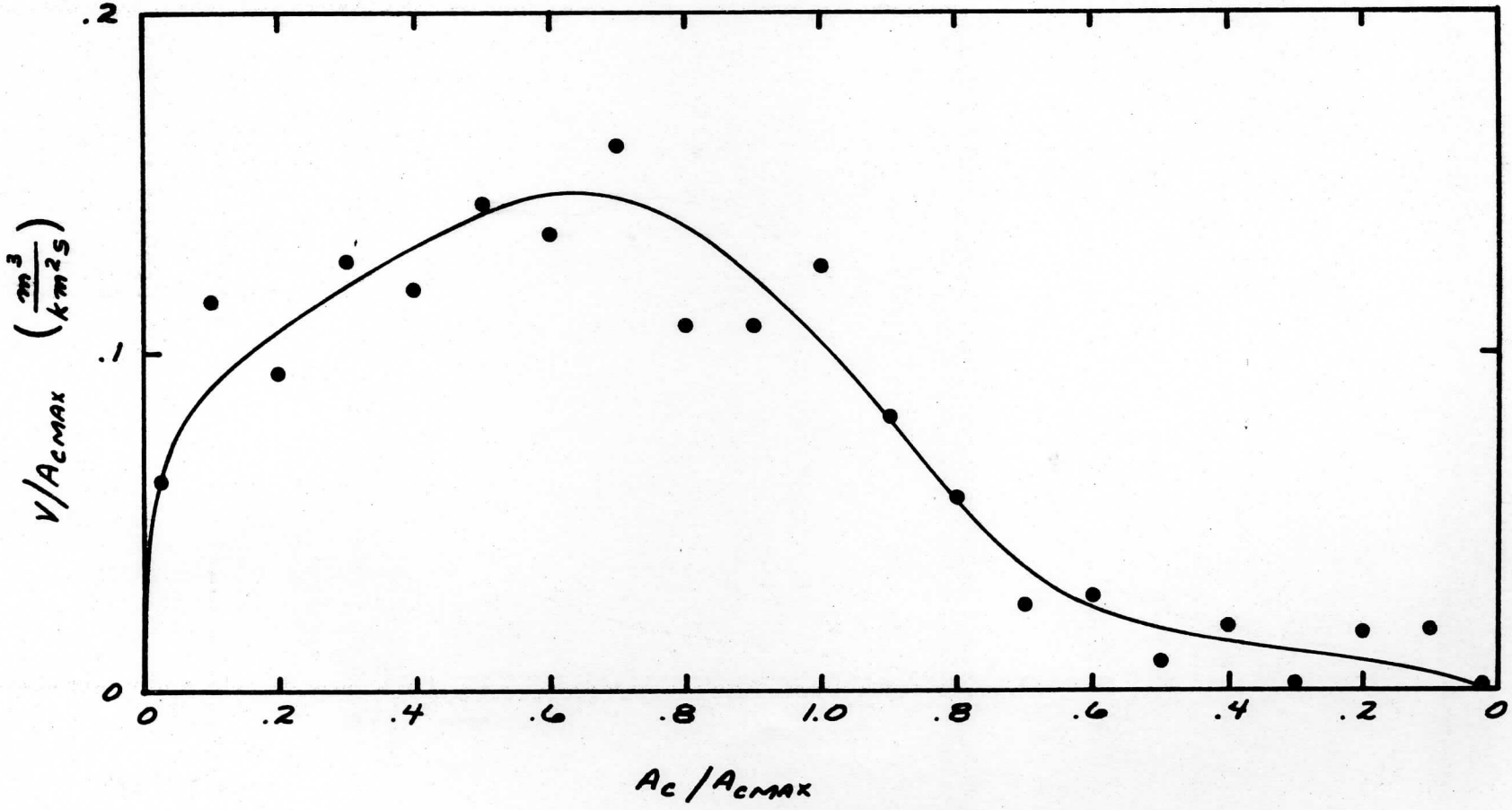

Figure 1

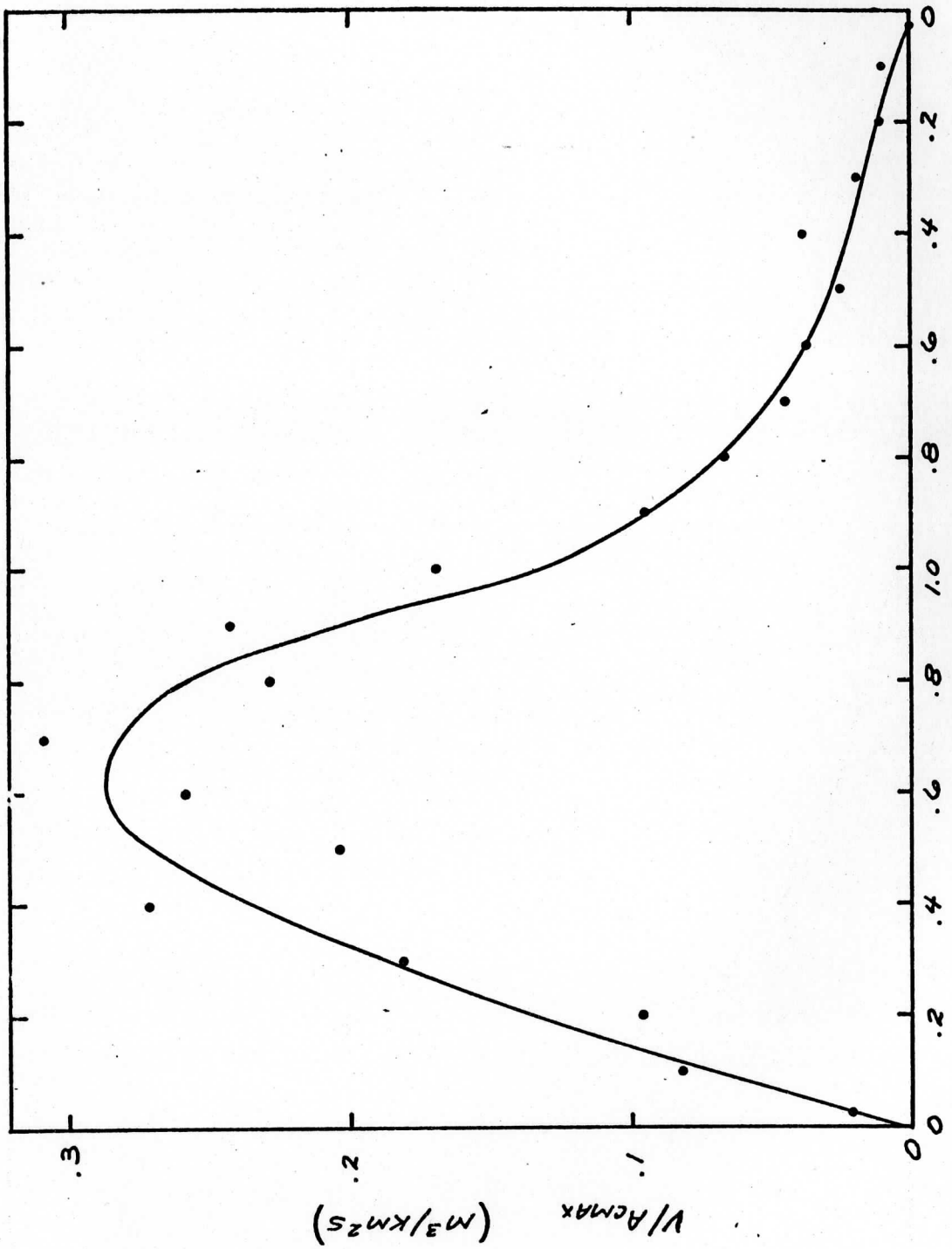

Figure 2

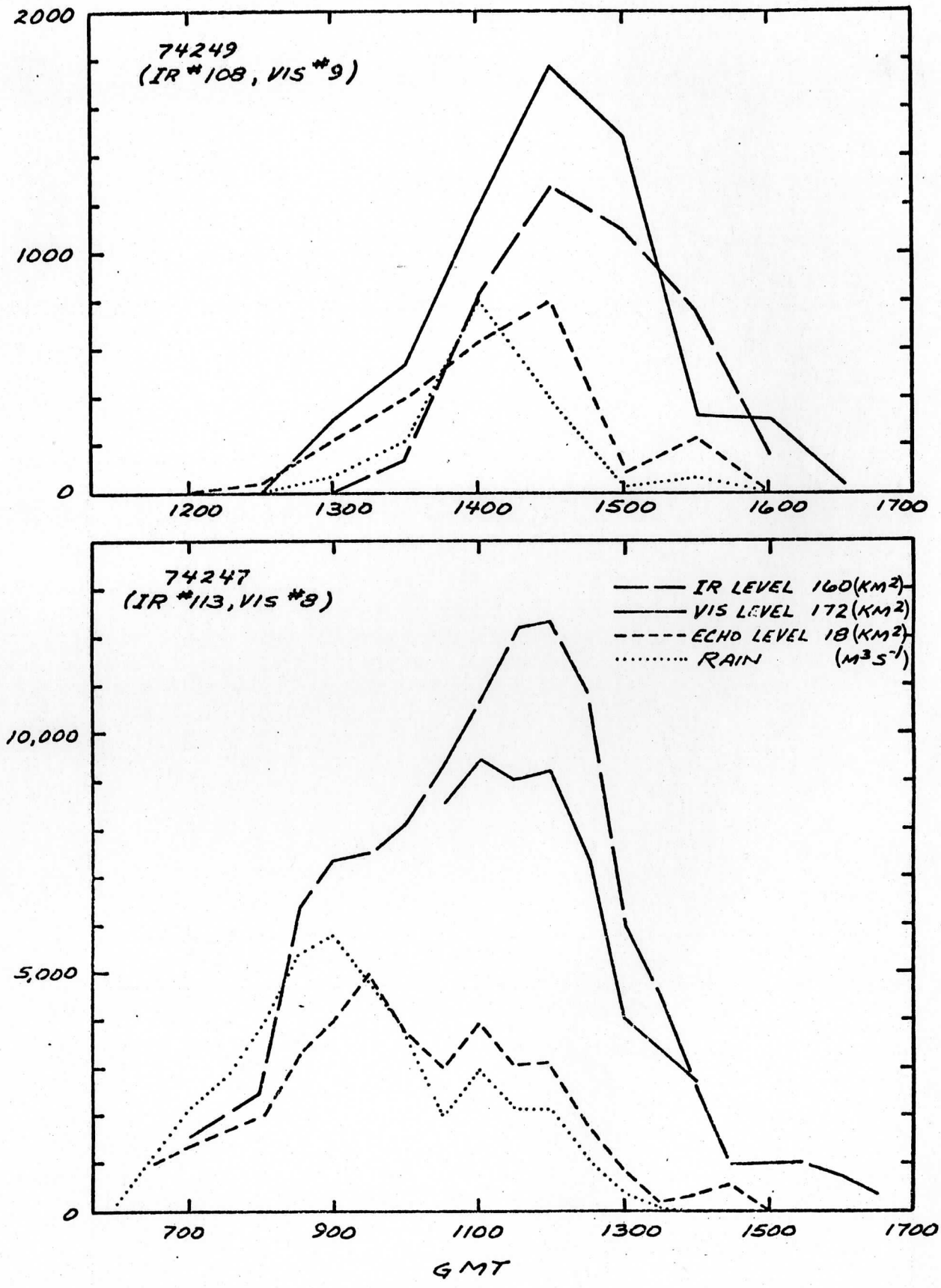
74249
(IR #108, VIS #9)
2000
1000
0
1200
1300
1400
1500
1600
1700
74247
(IR #113, VIS #8)
IR LEVEL 160(KM²)
VIS LEVEL 172(KM²)
ECHO LEVEL 18(KM²)
RAIN (M³S⁻¹)
10,000
5,000
0
700
900
1100
1300
1500
1700
GMT

Figure 3

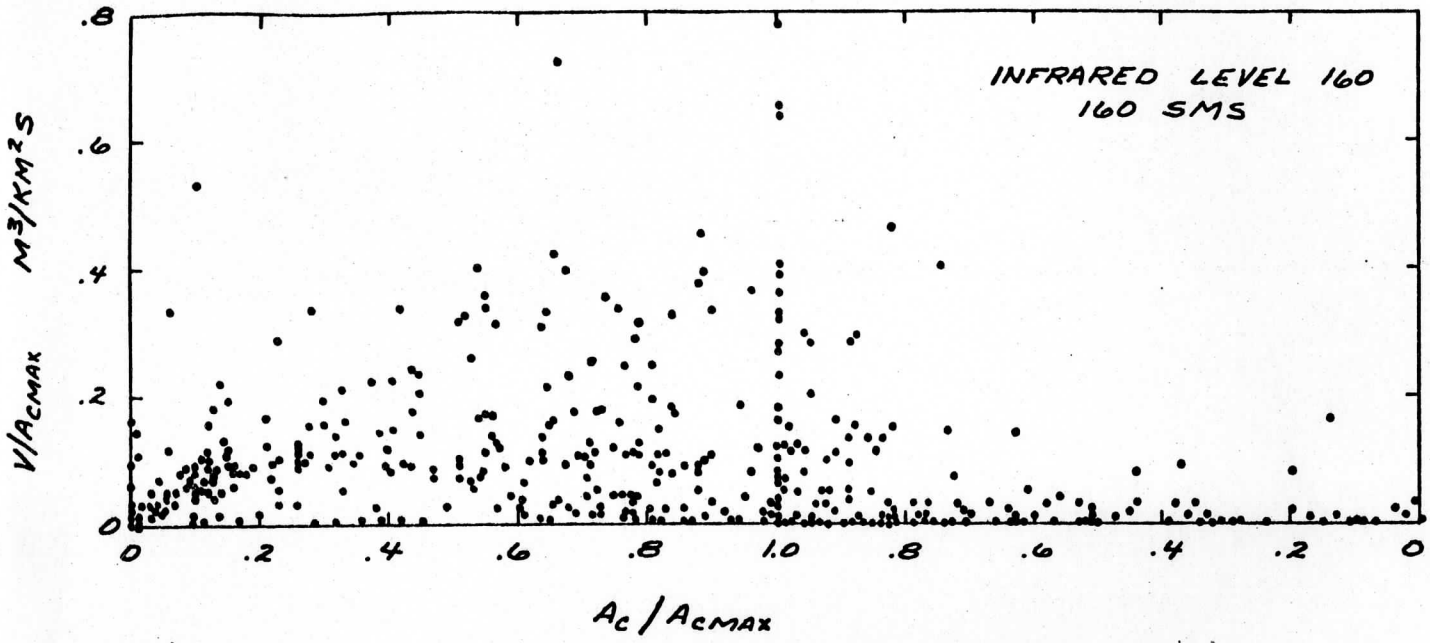
INFRARED LEVEL 160
160 SMS
V/ACMAX M³/KM²S
.8
.6
.4
.2
0
0 .2 .4 .6 .8 1.0 .8 .6 .4 .2 0
AC / ACMAX

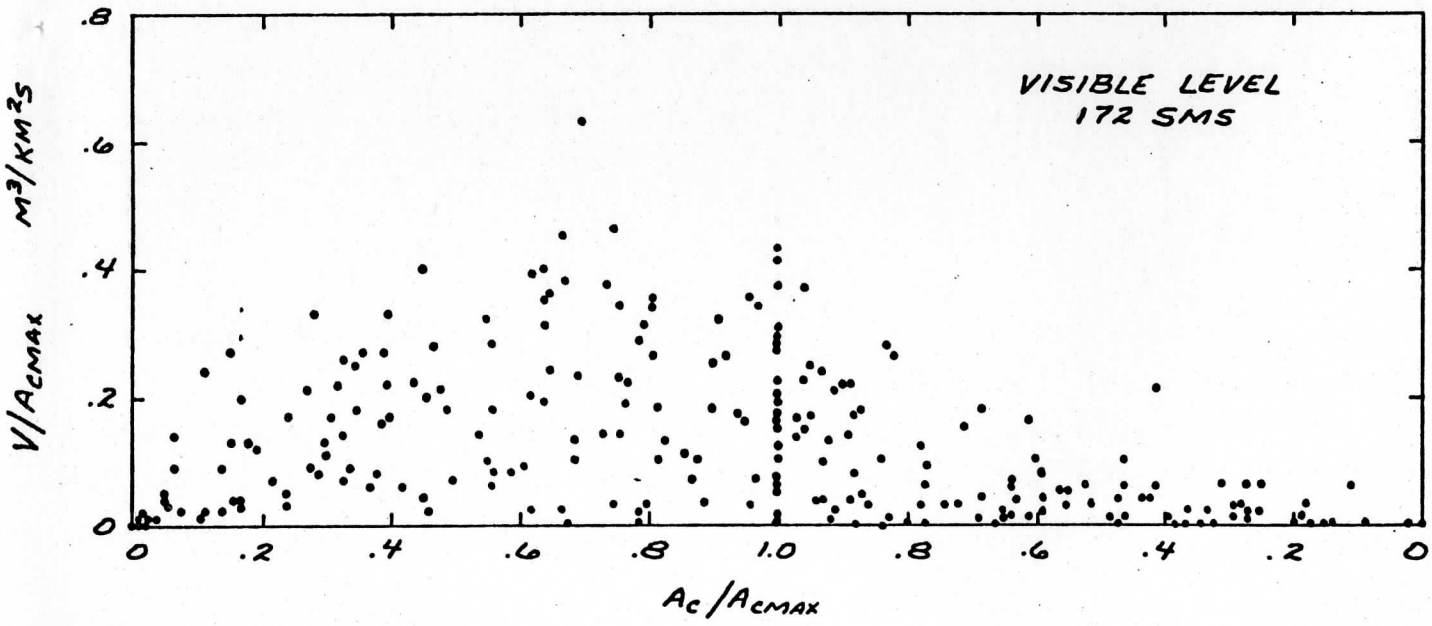
VISIBLE LEVEL
172 SMS
V/ACMAX M³/KM²S
.8
.6
.4
.2
0
0 .2 .4 .6 .8 1.0 .8 .6 .4 .2 0
AC / ACMAX

Figure 4

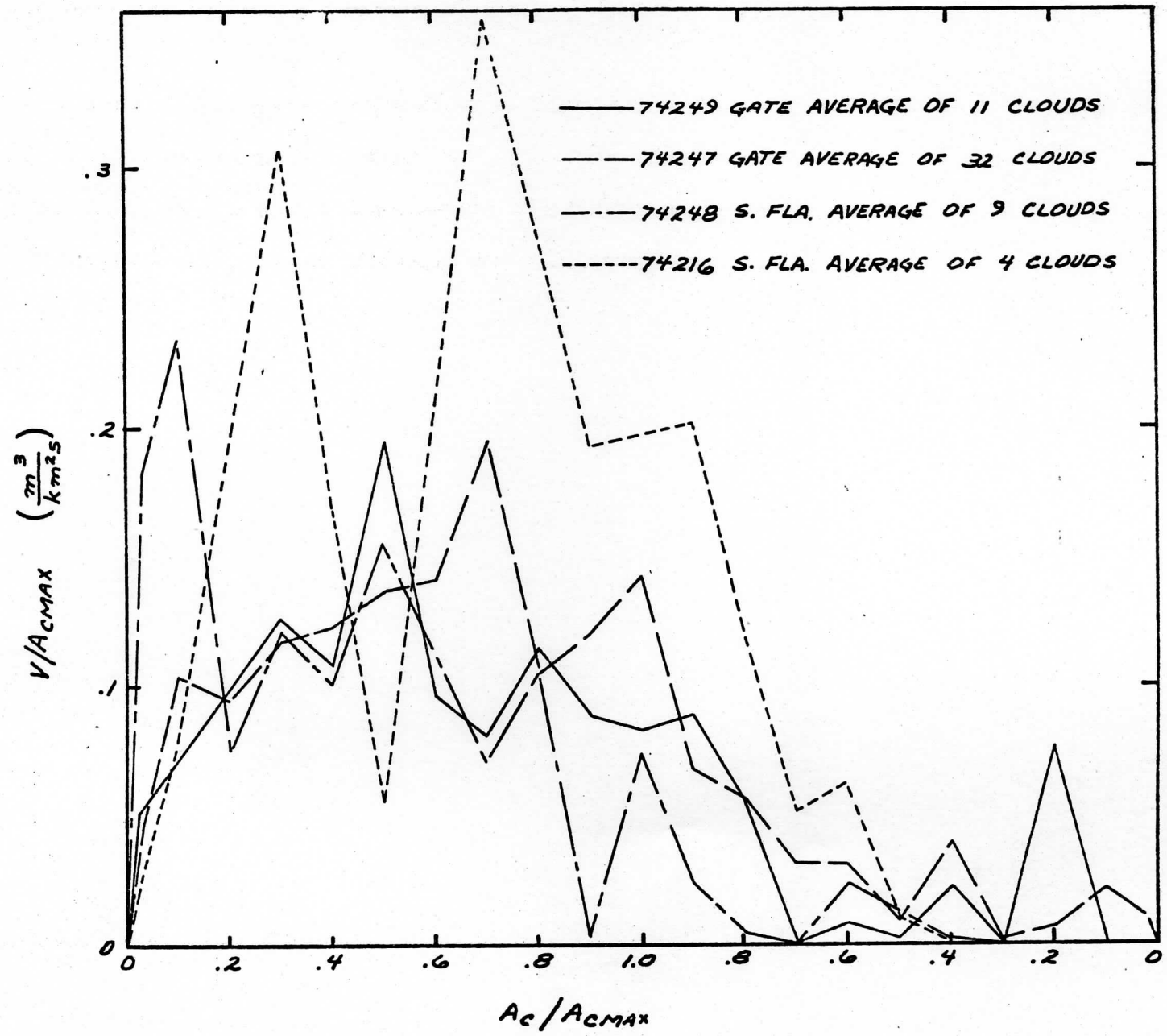
74249 GATE AVERAGE OF 11 CLOUDS
74247 GATE AVERAGE OF 32 CLOUDS
74248 S. FLA. AVERAGE OF 9 CLOUDS
74216 S. FLA. AVERAGE OF 4 CLOUDS
V/ACMAX (m³/km²s)
.3
.2
.1
0
0
.2
.4
.6
.8
1.0
.8
.6
.4
.2
0
AC/ACMAX

Figure 5

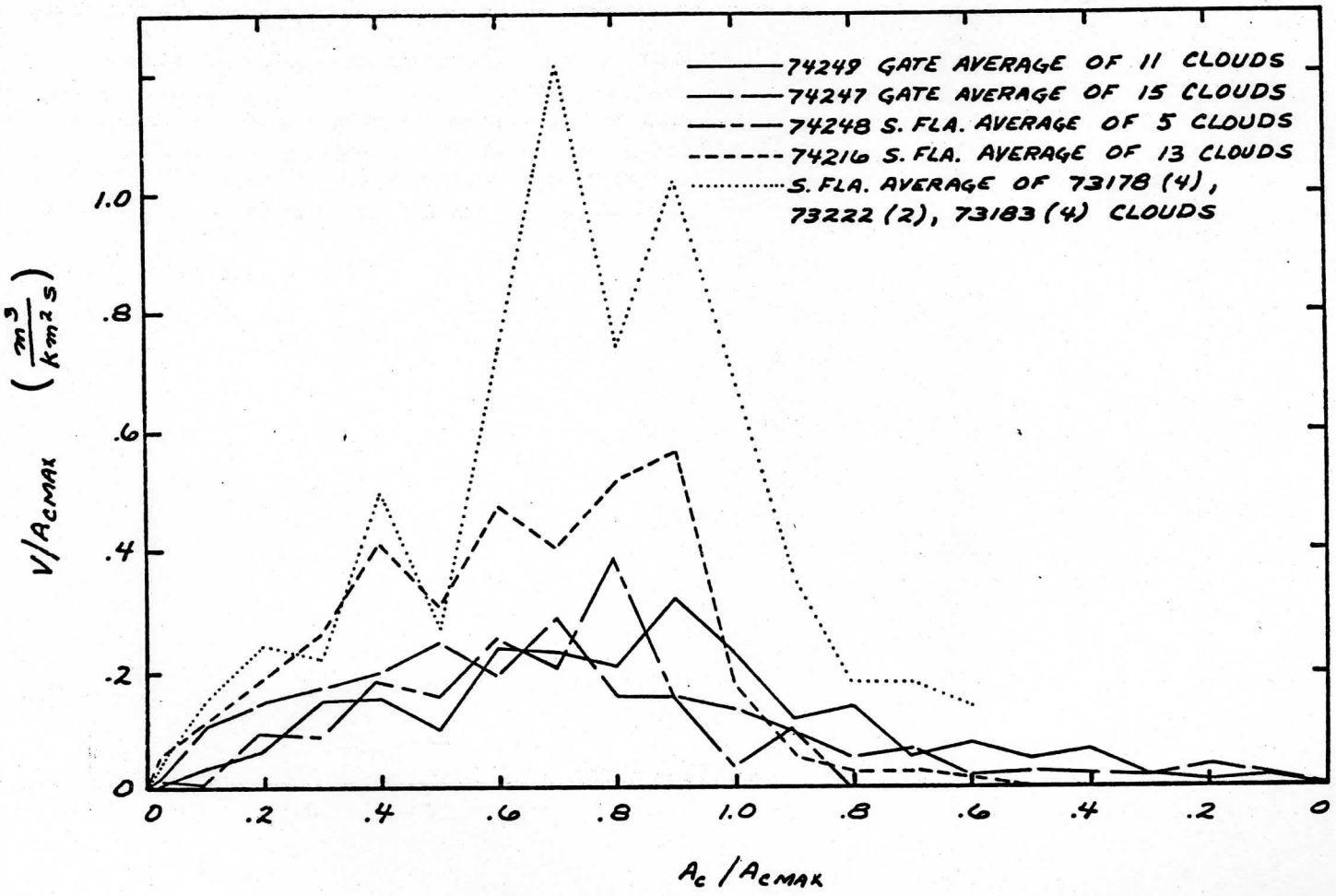
74249 GATE AVERAGE OF 11 CLOUDS
74247 GATE AVERAGE OF 15 CLOUDS
74248 S. FLA. AVERAGE OF 5 CLOUDS
74216 S. FLA. AVERAGE OF 13 CLOUDS
S. FLA. AVERAGE OF 73178 (4), 73222 (2), 73183 (4) CLOUDS
V/Ac MAX (m³/km² s)
1.0
.8
.6
.4
.2
0
0 .2 .4 .6 .8 1.0 .8 .6 .4 .2 0
Ac / Ac MAX

Figure 6

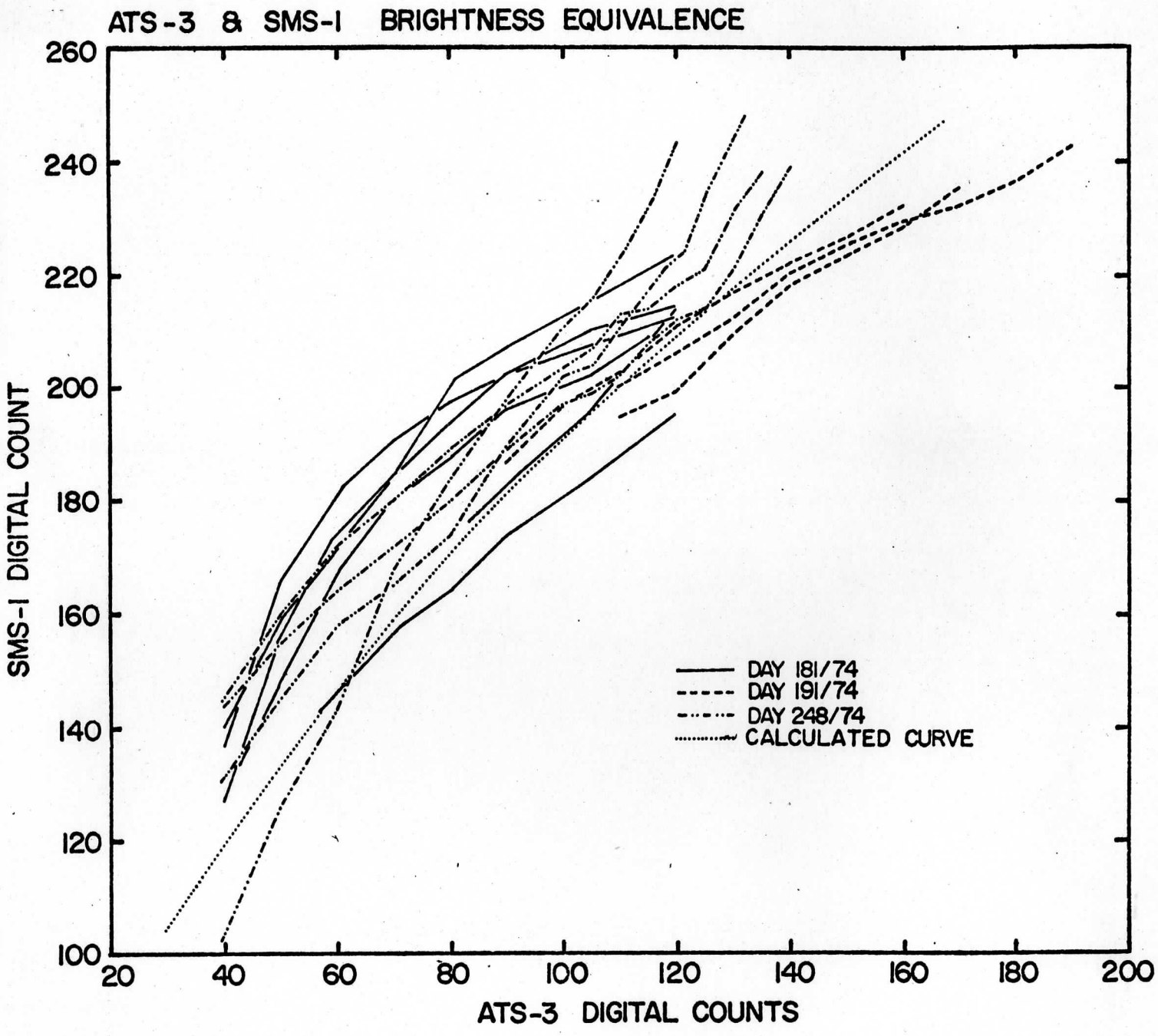
ATS-3 & SMS-1 BRIGHTNESS EQUIVALENCE
SMS-1 DIGITAL COUNT
260
240
220
200
180
160
140
120
100
20
40
60
80
100
120
140
160
180
200
ATS-3 DIGITAL COUNTS
DAY 181/74
DAY 191/74
DAY 248/74
CALCULATED CURVE

Figure 7

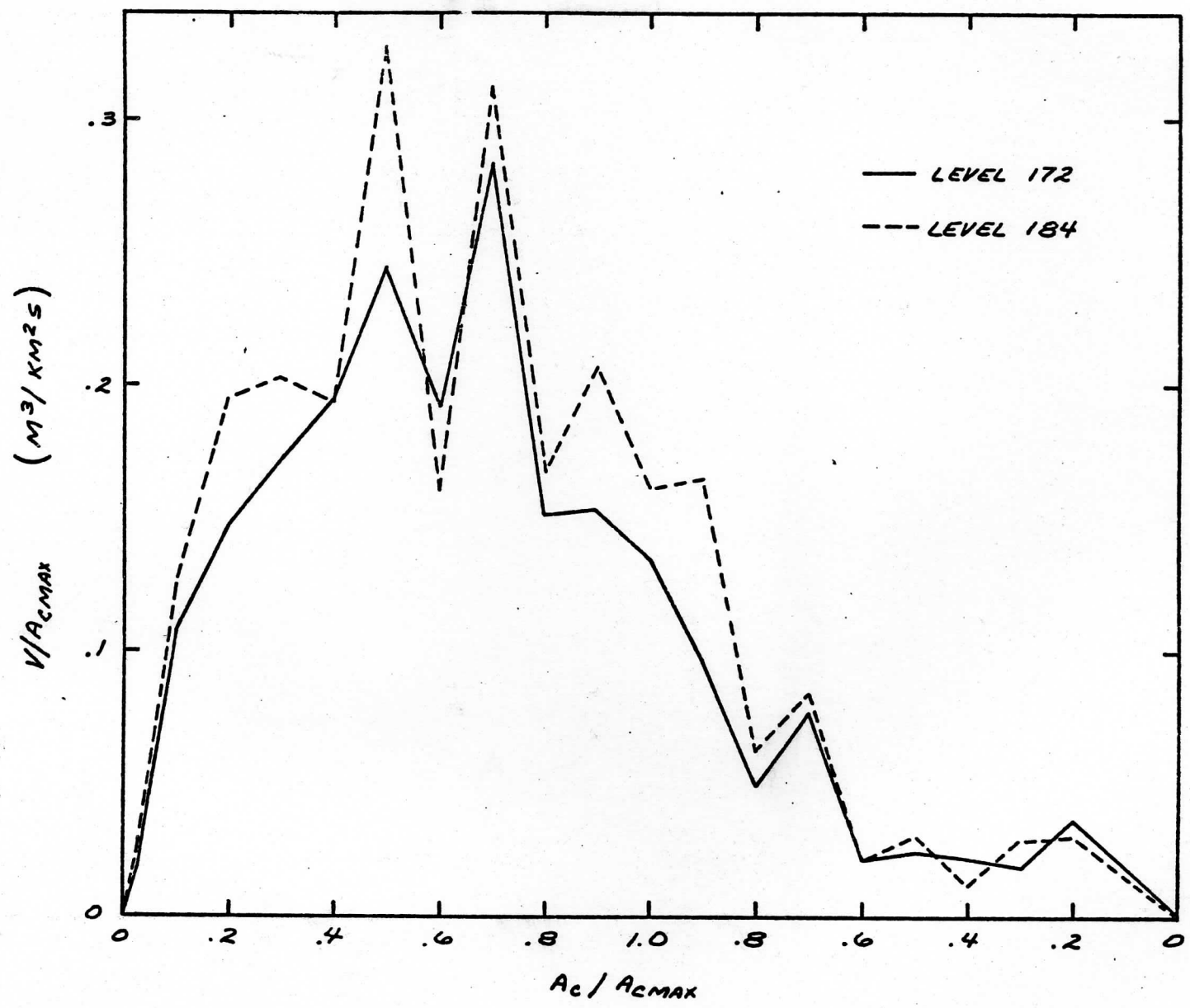
LEVEL 172
LEVEL 184
V/Acmax (m³/km²s)
Ac / Acmax
0
.1
.2
.3
0
.2
.4
.6
.8
1.0
.8
.6
.4
.2
0

Figure 8

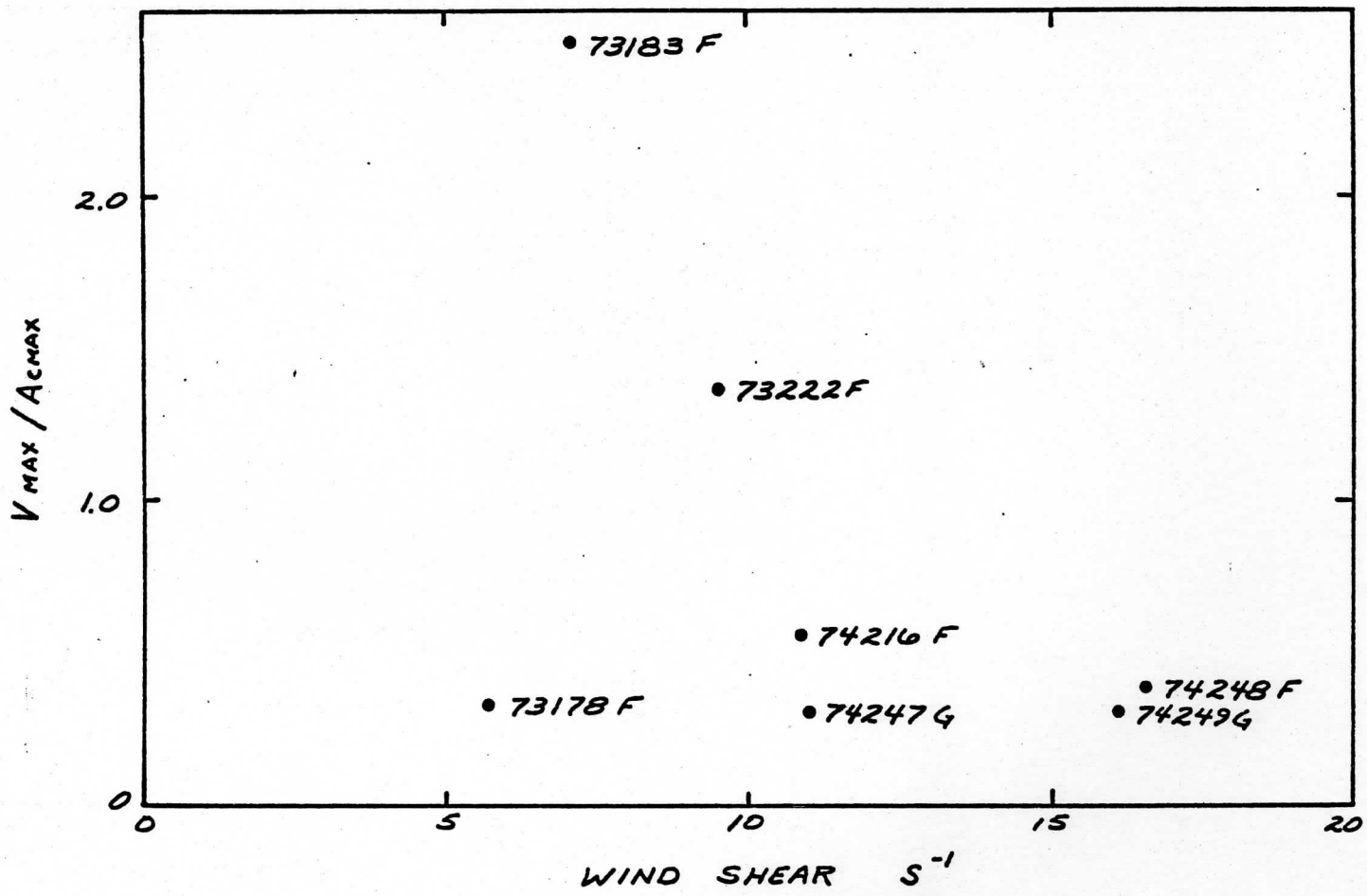
73183 F
73222F
74216 F
73178 F
74247 G
74248 F
74249G
2.0
1.0
0
0
5
10
15
20
V MAX / ACMAX
WIND SHEAR S-1

Figure 9

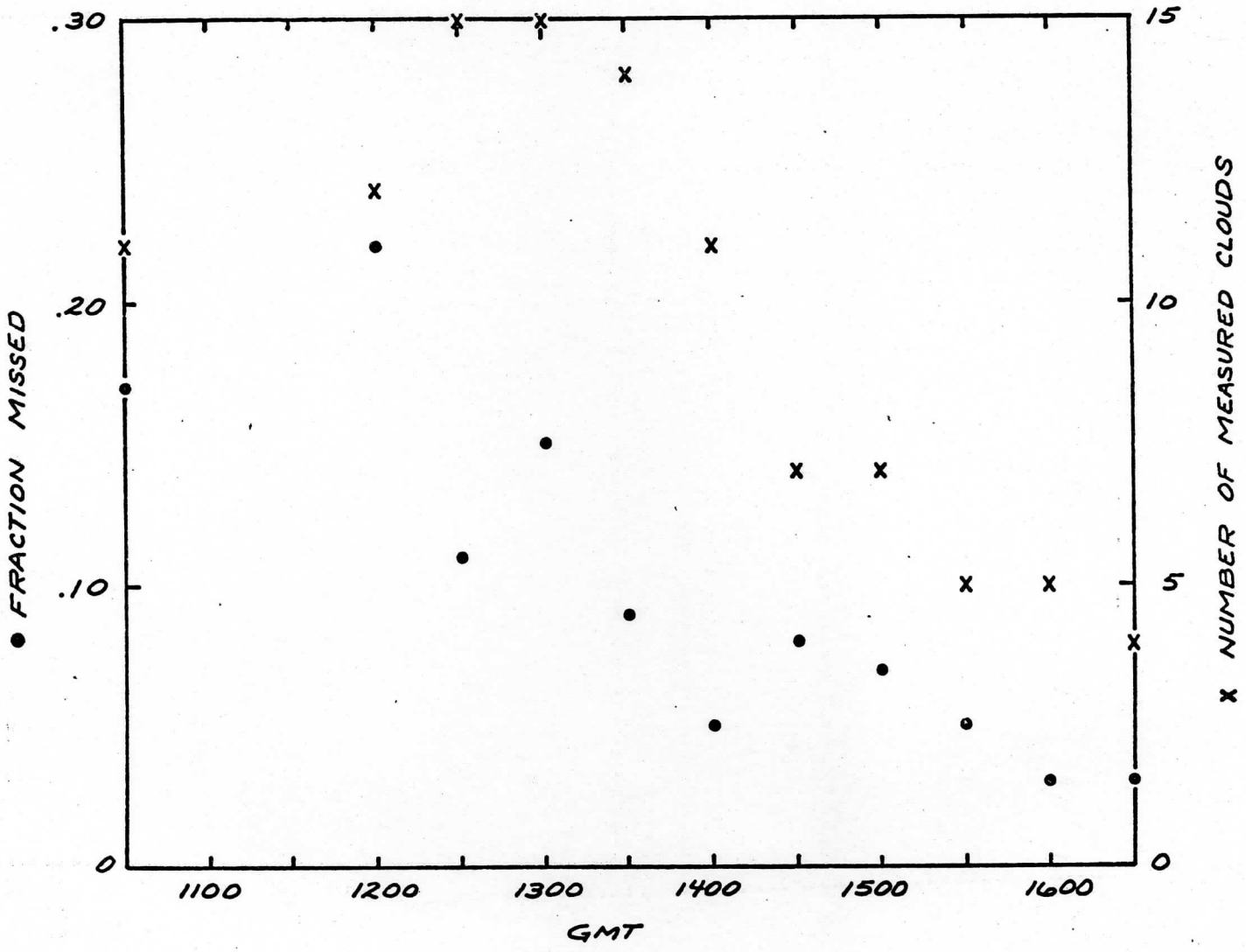
.30
.20
.10
0
15
10
5
0
1100
1200
1300
1400
1500
1600
GMT
● FRACTION MISSED
x NUMBER OF MEASURED CLOUDS

Figure 10

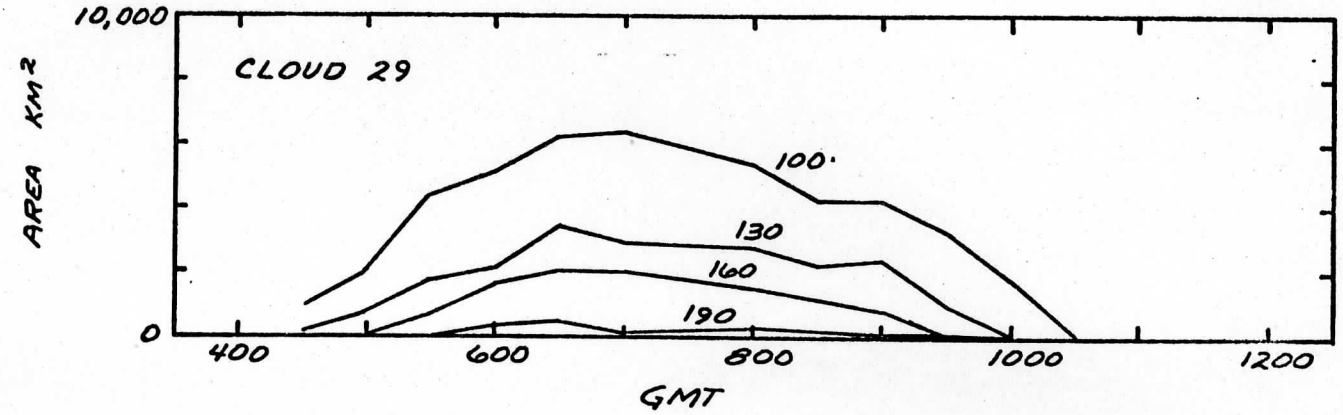
10,000
CLOUD 29
AREA KM²
100
130
160
190
0
400
600
800
1000
1200
GMT

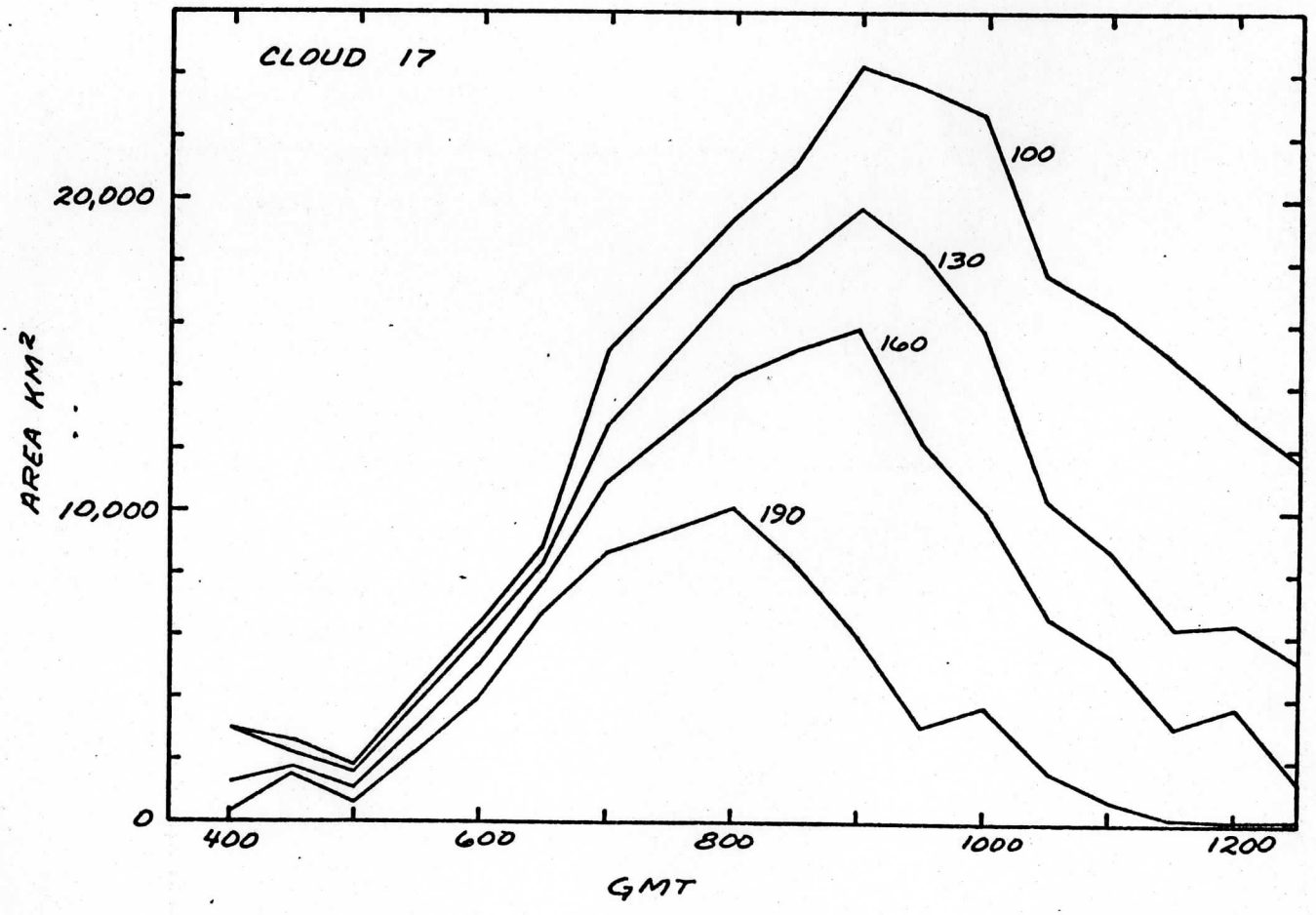
CLOUD 17
20,000
AREA KM²
10,000
100
130
160
190
0
400
600
800
1000
1200
GMT

Figure 11

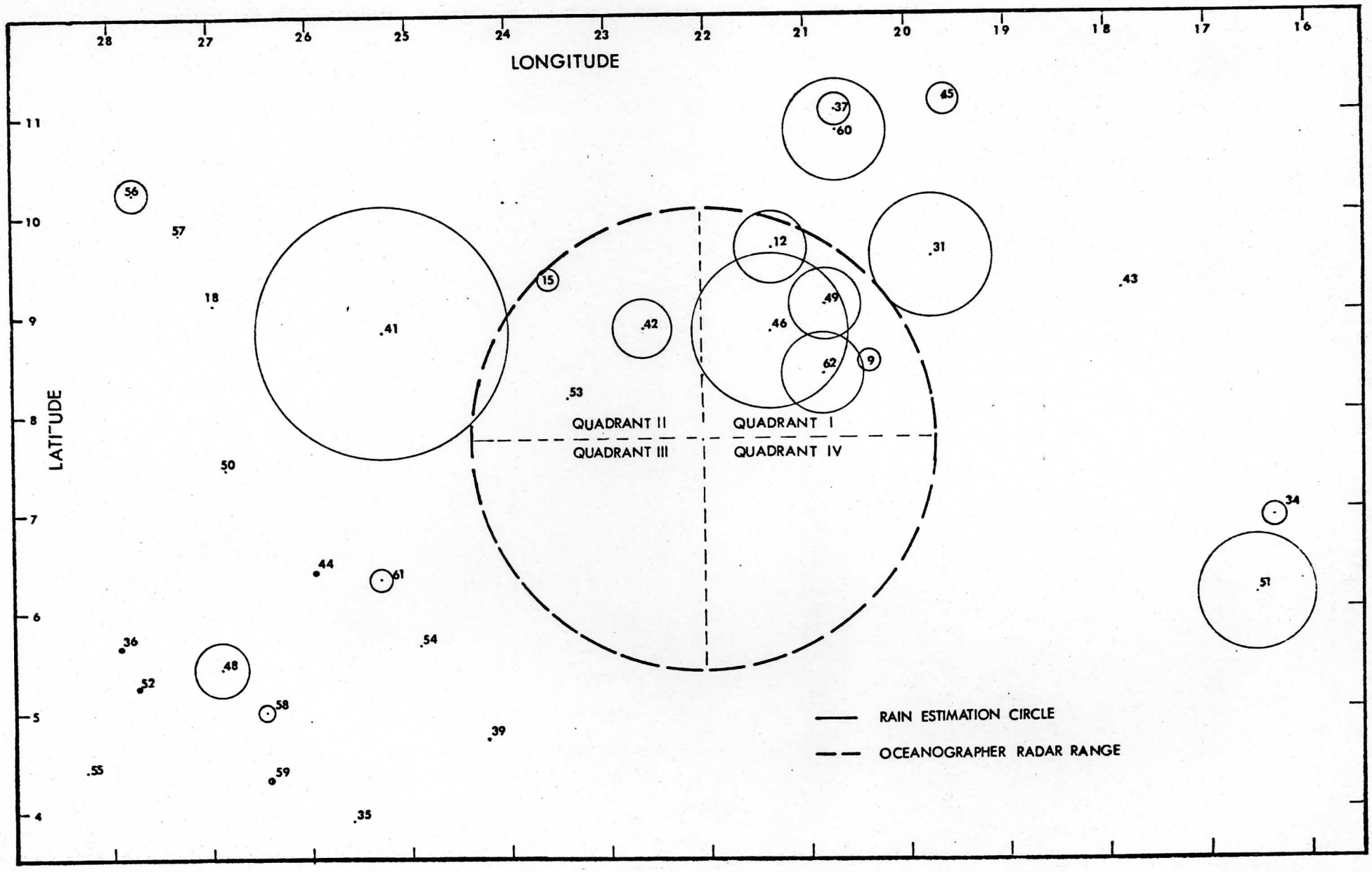
LONGITUDE
28
27
26
25
24
23
22
21
20
19
18
17
16
LATITUDE
11
10
9
8
7
6
5
4
QUADRANT II
QUADRANT I
QUADRANT III
QUADRANT IV
RAIN ESTIMATION CIRCLE
OCEANOGRAPHER RADAR RANGE
37
60
45
56
57
12
31
15
18
43
49
41
42
46
62
9
53
50
34
44
61
51
36
54
48
52
58
39
55
59
35

Figure 12

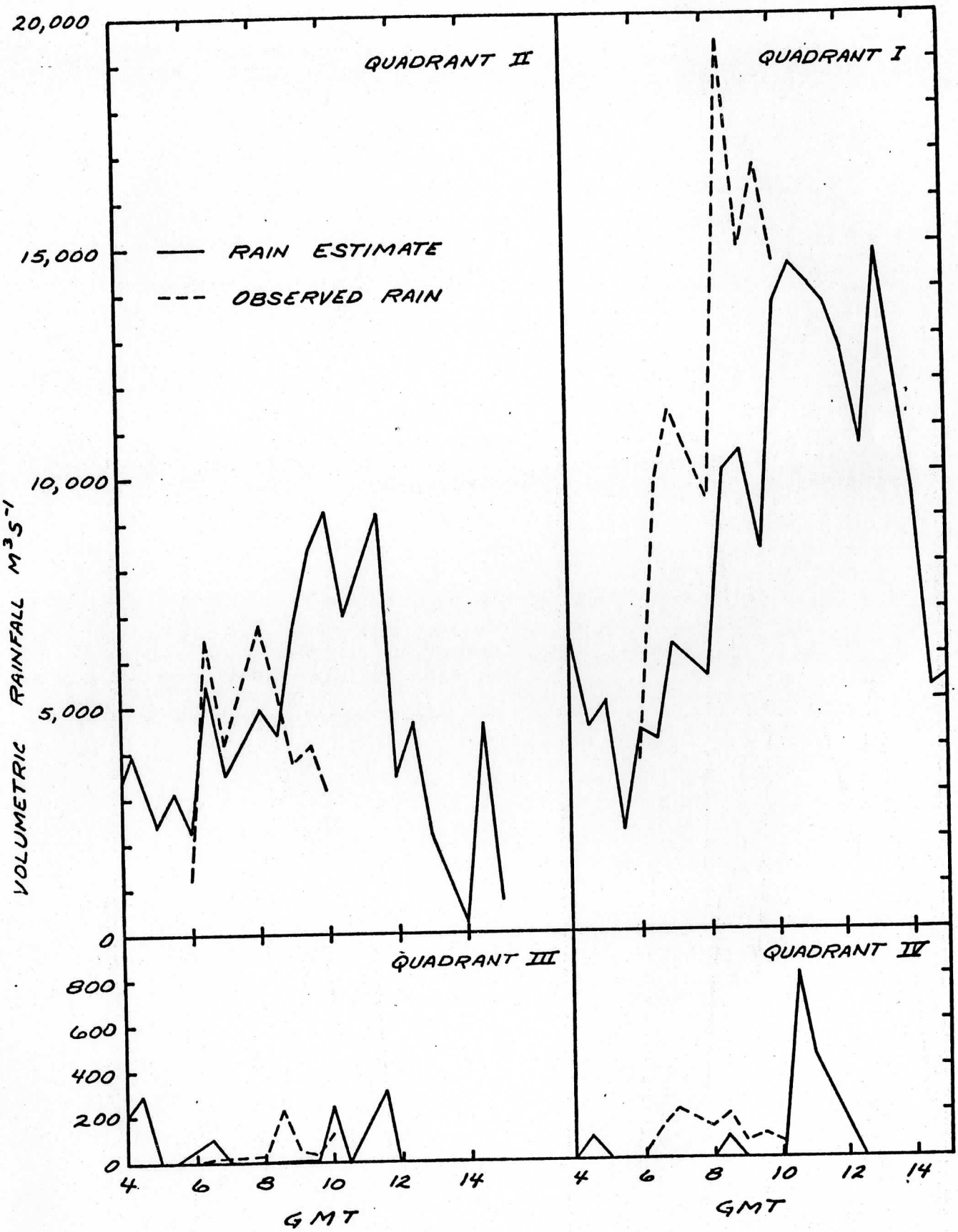
20,000
15,000
10,000
5,000
0
QUADRANT II
QUADRANT I
QUADRANT III
QUADRANT IV
RAIN ESTIMATE
OBSERVED RAIN
VOLUMETRIC RAINFALL M³S⁻¹
800
600
400
200
0
4
6
8
10
12
14
GMT
GMT

Figure 13

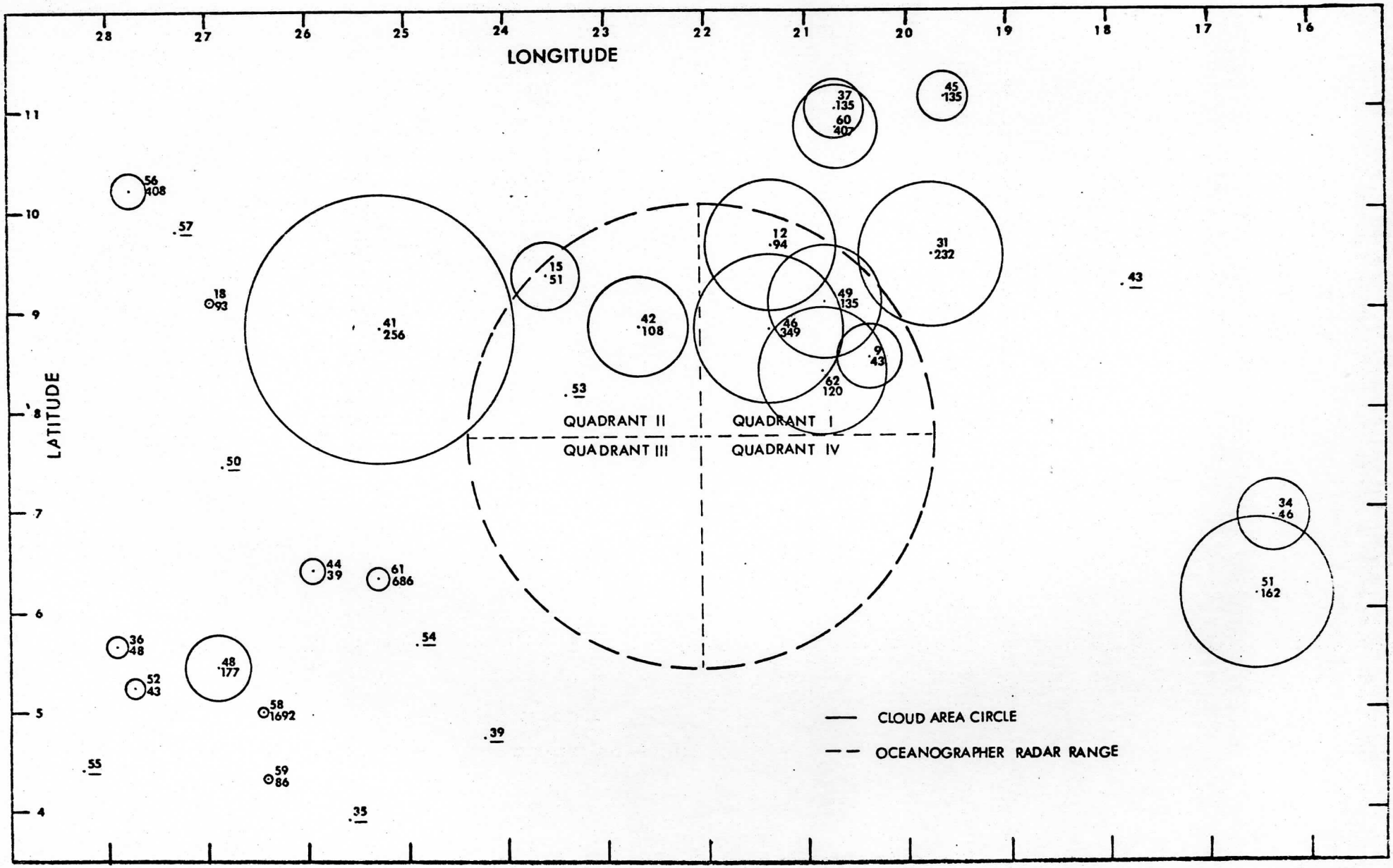
LONGITUDE
28
27
26
25
24
23
22
21
20
19
18
17
16
LATITUDE
11
10
9
8
7
6
5
4
37
135
60
407
45
135
56
408
57
12
94
31
232
15
51
18
93
41
256
42
108
43
49
135
46
349
9
43
62
120
53
QUADRANT II
QUADRANT I
QUADRANT III
QUADRANT IV
50
34
46
44
39
61
686
51
162
54
36
48
48
177
52
43
58
1692
39
55
59
86
35
CLOUD AREA CIRCLE
OCEANOGRAPHER RADAR RANGE

Figure 14

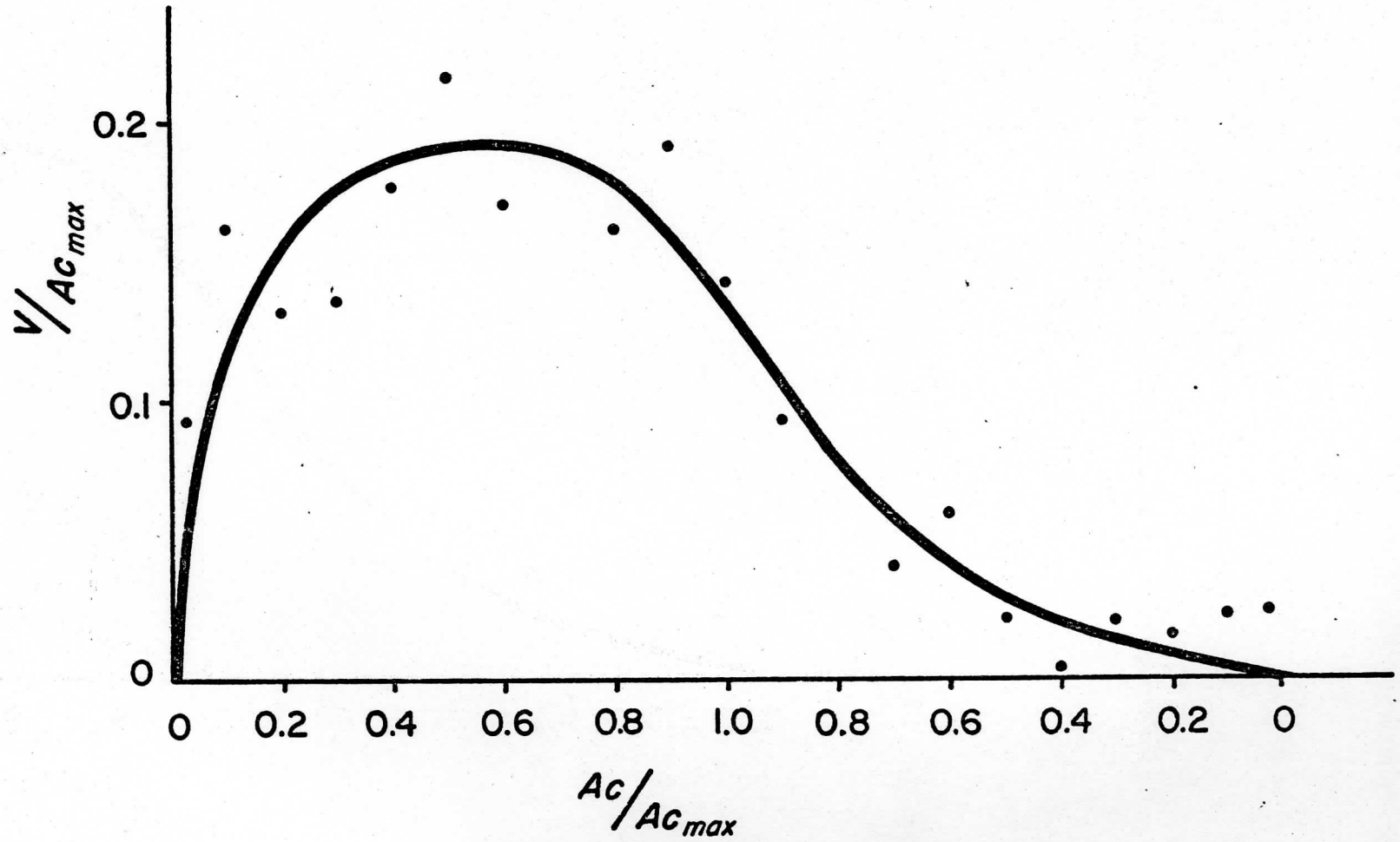

Figure 15

APPENDIX A: GATE RADAR CHARACTERISTICS

The calculation of rainfall from GATE radar data differs in several respects from calculations over South Florida. Whereas a 10 cm radar was used over Southern Florida, the GATE radar was 5 cm, and therefore more susceptible to attenuation by heavy precipitation.

Rainfall calculations initially were made with a provisional rainfall reflectivity (Z-R) suggested by Hudlow (personal communication, 1976). This relationship, $Z = 300\ R^{1.3}$, recently was revised. The accepted GATE Z-R relation now is $Z = 232\ R^{1.25}$ (Austin et al., 1976).

Except for the 5 September test case, the figures in this report show rainfall calculated with the new Z-R relation. The test case rain estimations (Fig. 12, Fig. 13, Fig. 14, Table 2) were made from a normalized cloud area and rainfall graph (Fig. 15) calculated with the old Z-R. The verification rainfall in Fig. 13 was also calculated with the old Z-R.

The preliminary GATE radar data used throughout had not been corrected for atmospheric attenuation, rain attenuation, rain on the radome, and beam filling, all of which contribute to underestimates of rainfall. Data sets corrected for at least some of these problems will be released within the next few months. Changes from the set used here may require remeasurement of the rainfall and recalculation of the cloud area-rainfall relations.

APPENDIX B: RAINFALL CALCULATION FROM GATE RADAR TAPE

Rainfall was calculated from the GATE Oceanographer Radar Hybrid Work Tape. The tape contained decibels of reflectivity, intensity resolution 1 dbz, range 0-63, spacial resolution 4 km by 4 km. Rain is calculated from the GATE rainfall-reflectivity relation, ~~$Z = 232\ R^{12.5}$~~ $Z = 232\ R^{1.25}$. Since $D = 10 \log_{10} Z$, this yields

$$R = \frac{10^{D/12.5}}{78.053}$$

where D = digital level on tape, Z = reflectivity in $mm^6\ m^{-3}$, and R = rain rate in $mm\ hr^{-1}$. Using McIDAS, the area of an echo between successive levels is measured. The median level is used to calculate rain rate for that level interval. The sum of area times rain rate times ($1000\ m\ mm^{-1}\ km^{-2}$) times $[hr(3600\ s)^{-1}]$ for the whole range of levels is volumetric rainfall in $m^3\ s^{-1}$. Threshold areas at eight decibel levels (6, 12, 18, 24, 30, 36, 42, 48) were used for 6 September, and sixteen levels (10, 18, 21, 24, 27, 30, 33, 36, 39, 42, 45, 48, 51, 54, 57, 60) for 4 and 5 September.